BREAST IMAGING

I J Radiol. 2023 July; 20(3):e136102. https://doi.org/10.5812/iranjradiol-136102.

Published online 2023 October 6. **Systematic Review**

Application of Elastography in the Diagnosis of Idiopathic Granulomatous Mastitis (IGM): A Systematic Review

Seyyed Mohammad Hosseini [1], Masoumeh Gity [2,*], Parham Talebi Boroujeni [2], Mona Asghari Ahmadabad [3] and Ali Jahanshahi [3]

[1] Faculty of Medicine, Shahed University, Tehran, Iran
[2] Advanced Diagnostic Interventional Radiology Research Center, Tehran University of Medical Sciences, Tehran, Iran
[3] Faculty of Medicine, Guilan University of Medical Sciences, Rasht, Iran

[*] *Corresponding author*: Advanced Diagnostic Interventional Radiology Research Center, Tehran University of Medical Science, Tehran, Iran. Email: p_gity@yahoo.com

Received 2023 March 04; **Revised** 2023 September 02; **Accepted** 2023 September 09.

Abstract

Context: Idiopathic granulomatous mastitis (IGM) is a benign inflammatory condition of the breasts with an unknown etiology, which can mimic breast cancer on conventional ultrasound (US). Other imaging modalities, such as mammography and magnetic (MRI) resonance imaging, cannot efficiently differentiate this condition from malignancies. Elastography is a novel imaging technique used to evaluate tissue elasticity.

Objectives: This systematic review aimed to investigate the imaging features of IGM on elastography and also to determine whether this modality is useful for distinguishing IGM from other breast lesions.

Methods: A comprehensive literature search was conducted across several databases, including Medline, Embase, Cochrane Library, Scopus, and Web of Science, in October 2022. The Joanna Briggs Institute (JBI) critical appraisal tool was used for the quality assessment of the studies.

Results: After screening 851 articles, seven studies investigating ultrasound elastography (USE) were found to meet the inclusion criteria. Regarding the quantitative findings, both the strain ratio (SR) and shear wave velocity (SWV) were observed to be higher in malignant masses as compared to IGM. Additionally, qualitative scoring systems, such as the Tsukuba and Tozaki classifications, assigned higher scores to malignant lesions. Five of the included studies in this review proposed a specific cut-off point for differentiating IGM from malignancies, using either SWV, SR, or elasticity scores (ES). In four of the studies, these criteria exhibited sensitivity and specificity of approximately 90%.

Conclusion: The current findings suggest that USE can serve as a valuable tool for distinguishing IGM from breast malignancies. By potentially reducing the number of unnecessary tissue biopsies, this modality may lead to a more efficient patient evaluation process.

Keywords: Idiopathic Granulomatous Mastitis, Elastography, Breast, Malignancy

1. Context

Idiopathic granulomatous mastitis (IGM) is a chronic benign inflammatory disease, marked by the development of non-caseating granulomas within the lobules of the mammary glands (1). Kessler and Wolloch have introduced this condition as a significant differential diagnosis for lesions associated with breast carcinoma (2). While the precise etiology of IGM remains unknown, it is postulated that the disease may have an autoimmune origin. Typical manifestations of IGM include breast masses, which are often accompanied by axillary lymphadenopathy, nipple inversion, the formation of sinuses and abscesses, and the ulceration of the breast skin (1). These symptoms are also common in malignant breast lesions, which can lead to some cases of IGM being erroneously diagnosed as cancer (3).

While histological confirmation is critical for the diagnosis of IGM (4), different imaging modalities have been also used in previous studies to detect IGM. Mammography, as a screening tool, cannot distinguish IGM from other pathologies (5). In magnetic resonance imaging (MRI), a ring-shaped enhancement is the most common pattern of IGM, although it has low specificity for diagnosis (4, 6). Moreover, ultrasonography (US) typically

presents IGM as a hypoechoic lesion and may detect sinus tract and lymph node enlargement (1, 4).

Elastography is a technique that evaluates the quality or quantity of tissue elasticity (7). This technique is divided into two main categories of ultrasound elastography (USE) and magnetic resonance elastography (MRE). Two methods are available for USE, including shear wave elastography (SWE) and strain elastography. During strain elastography, stress is applied to the tissue either externally by the operator or internally due to physiological processes, such as breathing or heartbeats. Meanwhile, an alternative method, known as acoustic radiation force impulse (ARFI) strain imaging, can be utilized, where an acoustic pulse is applied to induce tissue displacement (7).

Given that no current imaging modality has demonstrated satisfactory performance in detecting IGM, elastography can be a potentially useful tool, as it can enhance the efficiency of investigating IGM lesions and also aid in differentiating between IGM and other conditions, such as cancers. To the best of our knowledge, this study is the first systematic review on this subject.

2. Objectives

The objective of this study was to systematically review all research that has explored the application of USE in the evaluation of IGM lesions. This study also aimed to describe the characteristics of IGM as observed on USE and to investigate the accuracy of USE in distinguishing IGM from other types of breast lesions (i.e., malignancies).

3. Methods

3.1. Study Protocol and Registration

The current review method is compatible with the Preferred Reporting Items for Systematic Reviews and Meta-Analyses (PRISMA) guidelines (8) and is available on the International Prospective Register of Systematic Reviews (PROSPERO) website (CRD42022325968).

3.2. Selection Criteria

The selection criteria for the articles were formulated based on the Patient/Problem, Intervention, Comparison and Outcome (PICO) criteria. The patients were defined as women with a biopsy-proven IGM mass. The elastography techniques were considered as the diagnostic intervention. Regarding comparison, the current review investigated all studies using USE for the assessment of IGM lesions. Some of these studies were descriptive and only reported the features of IGM lesions on USE. For these studies, no comparison was defined, and the IGM patients were recruited based on tissue biopsy. Moreover, some studies reported IGM features on USE and also assessed the efficacy of USE in distinguishing IGM from other conditions (e.g., malignancies). For these studies, the comparator was defined as the gold standard diagnostic test (i.e., tissue biopsy) for distinguishing IGM from other lesions. Finally, the outcome was defined as the diagnostic assessment parameters of elastography techniques, such as accuracy and area under the curve (AUC).

The exclusion criteria were non-original papers (e.g., conference papers and abstracts, case reports, letters, book chapters, and narrative reviews), non-English papers, studies without accessible full-text manuscripts, and undesirable study settings (i.e., studies that did not use elastography or studies assessing breast lesions other than IGM).

3.3. Literature Search Strategy

In October 2022, two independent reviewers conducted a systematic search across Medline (via PubMed), Embase, Cochrane Library, Scopus, and Web of Science. The search utilized relevant keywords, such as ("idiopathic granulomatous mastitis" OR "granulomatous mastitis") AND ("elasticity imaging" OR "elastography" OR "elasticity imaging techniques" OR "sonoelastography" OR "ultrasonography" OR "ultrasound elastography" OR "shear wave elasticity imaging" OR "SWEI" OR "supersonic shear imaging" OR "acoustic radiation force impulse imaging" OR "ARFI" OR "transient elastography" OR "quasi-static elastography" OR "strain elastography"). No date or language limitation was considered in the primary search. Moreover, a manual search was conducted on Google Scholar, and the references of the most pertinent articles were screened to ensure that all relevant articles were included.

3.4. Screening and Data Extraction

The titles and abstracts of articles were independently reviewed by two researchers. Subsequently, the full-text manuscripts of the selected articles were separately reviewed by the same researchers. Each researcher compiled a list of articles to be included in the study. The screening results obtained by the reviewers were compared to identify any discrepancies. In cases where conflicts arose, the final decision was deferred to a third, senior author. Additionally, data extraction was performed by four reviewers. The data extracted by each reviewer was cross-verified by another reviewer. In instances where discrepancies arose, a third reviewer was asked to make

the final decision. Any missing data in the included articles was noted as not available (N/A).

3.5. Quality Appraisal

According to the objective of this review, all the included articles had a cross-sectional design. As such, the articles that met the inclusion criteria were evaluated based on the Joanna Briggs Institute (JBI) checklist, which is specifically designed for analytical cross-sectional studies (9); a score out of eight was ascribed to each study. The quality appraisal was conducted by the same reviewers responsible for data extraction. Based on the JBI's checklist, studies that scored less than four (out of eight items) were excluded.

4. Results

Following the initial search, out of 851 papers identified, 528 articles were retrieved and screened. After reviewing the abstracts, 508 papers were excluded as they either did not report accessible IGM data, did not utilize USE, or reported unsuitable evidence types (e.g., narrative reviews and letters). Twenty full-text manuscripts were retrieved and carefully examined. Finally, seven articles met all the inclusion criteria and were incorporated into the data synthesis. Figure 1 presents the PRISMA diagram of the literature search (8). Interestingly, all the studies included in the review were conducted in Turkey and were published in the time frame of 2014-2020 (Table 1).

4.1. Quality Appraisal

According to the JBI's appraisal checklist (9), seven studies were included in this review. One study (13) received a score of five out of eight due to some methodological limitations, such as the absence of a detailed description of participants and study setting. Four studies (10, 14-16) obtained a score of six out of eight, and two studies (11, 12) met all the checklist criteria.

4.2. Elastography Technique and Parameters

Among the studies included in this review, five detailed the findings of conventional US based on the breast imaging-reporting and data system (BI-RADS) score (11, 13-16). The remaining two studies reported the maximum diameter of the lesion, the type of lesion (10), as well as the size, shape, margin, echogenicity, and posterior acoustic features of the lesion (12) (Table 2).

The USE methods used in the included studies were strain elastography (10, 12, 13) and SWE (11, 14-16). The quantitative imaging parameters used in the included studies were the strain ratio (SR) (three studies) (10, 12, 13), and shear wave velocity (SWV) (four studies) (11, 14-16). Additionally, Tozaki (11, 14, 16) and Tsukuba elasticity scores (ES)(10, 13, 15) were calculated as qualitative imaging parameters.

4.3. Exclusive Studies on IGM

In a study by Durur-Karakaya et al. (10), the USE features of 27 IGM patients were described. Diffuse lesions were reported as the most prevalent lesions, followed by tubular lesions, masses, and cystic lesions, respectively. Mammography assessments in nine patients revealed no calcification or speculation. All ES scores ranged between one and three, while the SR was measured to be 1.10 ± 0.79 (mean ± SD). There was no variation in lesion size between USE and greyscale images in morphological assessments.

Additionally, Aslan et al. studied the association of SWE findings prior to treatment with the severity of IGM (14). Based on the symptom severity, they categorized the sample population into two groups. Patients with a focal disease, without fistula or serious abscess, were classified as the first group receiving conservative treatment with steroids. On the other hand, patients presenting with severe abscesses, fistulas, or a widespread disease were classified into the second group and received surgical treatment. However, their results indicated no significant association between the IGM severity and the SWV or BI-RADS categories.

4.4. USE Application for Distinguishing IGM from Cancerous Lesions

Five of the included studies, examining a total of 275 IGM and 377 breast cancer patients, investigated the utilization of USE for distinguishing malignancies from IGM. Table 3 presents the introduced cut-off points in each study, as well as the diagnostic accuracy.

Arslan et al. conducted a study to investigate the role of SR and ES in distinguishing between IGM and malignancies. They examined these parameters separately and in conjunction with B-mode US (13). The conventional US findings of IGM patients demonstrated that multiple irregular heterogeneous hypoechoic masses with a tubular extension and focal hypoechoic mass-like lesions with an indistinct border were the two most frequent patterns in B-mode US assessments. The combination of each imaging parameter with B-mode US for distinguishing IGM from malignant lesions increased specificity from 66.7% to 100%. Therefore, by integrating B-mode US assessment with SR and ES, higher sensitivity, positive predictive value (PPV), negative predictive value (NPV), and accuracy were achieved.

Moreover, Yagci et al. investigated the features of strain elastography in IGM lesions and evaluated its role

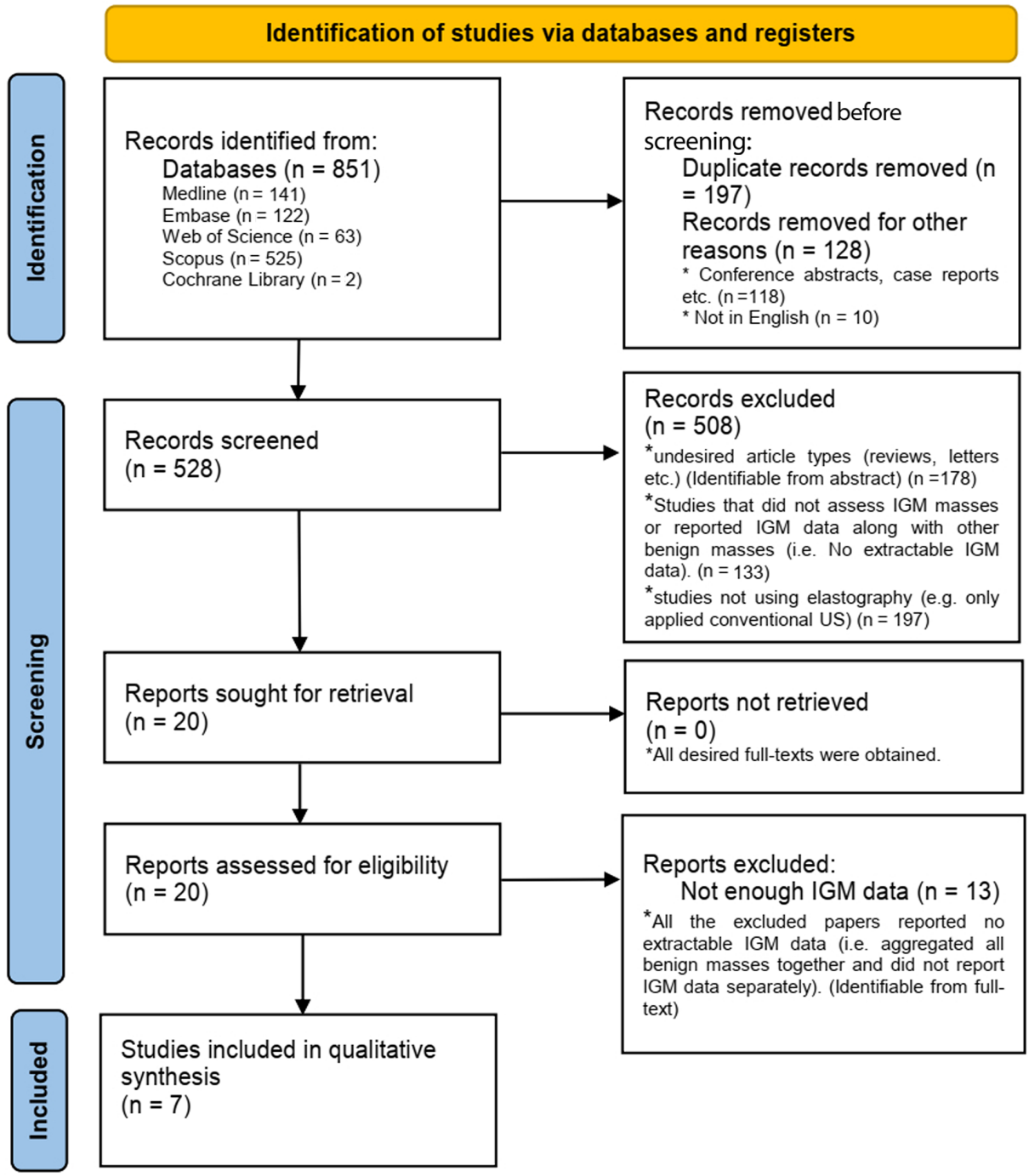

Figure 1. The PRISMA flow diagram of the study

Table 1. The Characteristics of the Included Studies

Authors	Year of publication	Number of participants	Age of participants	Objectives	Presenting symptoms	Type of modality	Device	Region of interest	Conventional US evaluation method	Quantitative USE parameter	Qualitative USE method
Durur-Karakaya et al. (10)	2014	IGM=27	IGM (37.8 ± 7.1 y)	Description of elastography findings for IGM	Palpable mass, breast pain, erythema, fistula formation, axillary lymphadenopathy, and failure to respond to treatment	Conventional US and strain elastography	EUB-6500; Hitachi® Medical, Tokyo, Japan	Breast and axilla	Maximum lesion diameter and lesion type (diffuse, tubular, mass, and cystic)	SR	Tsukuba classification
Teke et al. (11)	2016	IGM=4; Malignancy=122 (DCIS=9, IDC=98, ILC=10, malignant epithelial tumor=9)	IGM (39.5 ± 6.3 y); Malignancy (50.1 ± 9.7 y)	Differentiation between IGM and malignant breast masses	N/A	Conventional US and SWE	Acuson S2000 US system; Siemens Medical Solutions, Mountain View, CA, USA	Breast and axilla	BI-RADS score, tumor margin, shape, size, echo pattern, posterior acoustic features, and distribution	SWV	Tozaki classification
Yagci et al. (12)	2017	IGM=23; Malignancy=45 (IDC=42, ILC=2, malignant fibroepithelial tumor=1)	IGM (37.9 ± 6.6 y); Malignancy (52.8 ± 12.0 y)	Differentiation between IGM and malignant breast masses	N/A	Conventional US and strain elastography	Hi-Vision Preirus; Hitachi Medical Systems, Japan	Breast and axilla	Size, shape, margin, echogenicity, and posterior acoustic features	SR	N/A
Arslan et al. (13)	2018	IGM=77; Malignancy=36 (IDC=64, DCIS=5, ILC=4, mucinous carcinoma=2, medullary carcinoma=2)	IGM (35.6 ± 8.65 y); Malignancy (54.8 ± 11.8 y)	Differentiation between IGM and malignant breast masses	Palpable mass, breast pain, erythema, and nipple change	Conventional US and strain elastography	Aplio 500; Toshiba Medical Systems Corporation, Tokyo, Japan	Breast and axilla	BI-RADS score, tumor smargin, size, shape, echo pattern, posterior acoustic features, and distribution	SR	Tsukuba classification
Aslan et al. (14)	2018	IGM=39	Group 1 (conservative treatment): 38.44 ± 9.6 y; Group 2 (surgery): 36.05 ± 7.44 y	Analysis of the correlation between the severity of IGM and the pretreatment SWE findings	Palpable mass, erythema, nipple retraction, and sinus formation	Conventional US and SWE	Acuson S 2000; Siemens Medical Solutions, Mountain View, CA, USA	Breast	BI-RADS score	SWV	Tozaki classification
Makal and Guvenc (15)	2020	IGM=88; Malignancy=80	IGM (37± 9 y); Malignancy (49 ± 13 y)	Differentiation between IGM and malignant breast masses	Palpable mass, breast pain, erythema, nipple change, and abscess formation	Conventional US and SWE	Acuson S2000 Ultrasound System with Color Doppler Imaging; Siemens Healthcare, Erlangen, Germany	Breast	BI-RADS score, lesion location, and size	SWV	Tsukuba classification
Toprak et al. (16)	2020	IGM=39; Malignancy (IDC)=94	IGM (33.94 ± 6.29 y); Malignancy (50.58 ± 11.55 y)	Differentiation between IGM and malignant breast masses	N/A	Conventional US and SWE	Acuson S2000 US System; Siemens Medical Solutions, Mountain View, CA, USA	Breast	BI-RADS score, lesion size, shape, orientation, margin, echo pattern, posterior acoustic features, and calcifications	SWV	Tozaki classification

Abbreviations: IGM, idiopathic granulomatous mastitis; SR, strain ratio; ED, elastic diameter; DCIS, ductal carcinoma in situ; IDC, invasive ductal carcinoma; ILC, invasive lobular carcinoma; US, ultrasound; USE, ultrasound elastography; SWV, shear wave velocity; BI-RADS, breast imaging-reporting and data system; VTI, velocity time integral; SWE, shear wave elastography; y, year; N/A, not applicable (or available).

in distinguishing IGM from malignancies. The SR was 1.5 ± 0.8 in IGM patients and 5.3 ± 5.2 in cancer patients. They demonstrated that IGM patients had a significantly lower SR than malignant cases. They suggested 2.5 as an optimal cut-off point to differentiate IGM from cancerous lesions (12). Moreover, Makal and Guvenc assessed the application of SWE in differentiation of IGM from breast cancer. They found significantly higher SWE and BI-RADS scores in malignant cases. The SWV was considerably lower in IGM patients, and a cut-off point of 4.1 m/s was reported (15). Teke et al. also investigated how ARFI imaging can assist in discriminating between IGM and malignancies (11). A significant difference was found between the two subgroups in terms of marginal and internal SWV, and the values for these parameters were observed to be higher in patients diagnosed with cancer (Table 2). They concluded that supplementing conventional US with ARFI imaging would enhance the specificity.

Studies by Teke et al. and Makal and Guvenc indicated that the sensitivity and specificity of SWV for differentiating IGM from breast cancer exceeded 90% (11, 15). Toprak et al. specifically evaluated the sensitivity

Table 2. The Findings of The Included Studies

Authors	Conventional USE findings	Quantitative USE findings	Qualitative USE findings
Durur-Karakaya et al. (10)	Most common pattern: Diffuse. Mean maximum diameter of lesions: 24.74 ± 17.83 mm.	SR: 1.10 ± 0.79 (0.29 - 4.00).	Tsukuba score: 1.66 ± 0.55 (1.00 - 3.00)
Teke et al. (11)	Most common pattern: IGM: Irregular heterogeneous hypoechoic mass with tubular extensions and axillary adenopathy. Malignancy: Spiculated contours and posterior acoustic shadowing. IGM: BI-RADS 3 (n=18) and BI-RADS 4 (n=30). Malignancy: BI-RADS 3 (n=39) and BI-RADS 5 (n=83).	SWV: IGM: Internal SWV [2.76 (1.14 - 4.12)] (n=27); marginal SWV [3.19 (2.49 - 5.82)] (n=48); size (mm) [36 (7 - 135)] (n=48). Malignancy: Internal SWV [4.79 (2.12 - 8.02)] (n=73); marginal SWV [5.05 (2.09 - 8.46)] (n=122); size (mm) [25 (8 - 62)] (n=122).	Tozaki classification: IGM: Pattern 2 (n=2), pattern 3 (n=31), and pattern 4a (n=15). Malignancy: Pattern 3 (n=7), pattern 4a (n=34), and pattern 4b (n=81).
Yagci et al. (12)	Most common pattern: IGM: Irregular microlobulated contours and a heterogeneous hypoechoic structure. Malignancy: A heterogeneous hypoechoic structure with posterior acoustic shadowing.	SR: IGM: 1.5 ± 0.8 (0.2 - 4); Malignancy: 5.3 ± 5.2 (1.4 - 33).	N/A
Arslan et al. (13)	Most common pattern: IGM: An irregular heterogeneous hypoechoic mass with tubular extensions and unilateral axillary adenopathy. Malignancy: N/A. IGM: BI-RADS 3 (n=24) and BI-RADS 4 or 5 (n=12).	SR: IGM: 1.08 ± 0.58 (0.32-2.70); Malignancy: 4.71 ± 1.56 (1.18-7.53).	Tsukuba score: IGM: 1.36 ± 0.54 (1 - 3); Malignancy, 4.28 ± 1.01 (2 - 5).
Aslan et al. (14)	Group 1: Tubular hypoechoic structures (66.7%). Group 2: Tubular hypoechoic structures (57.2%). Group 1: BI-RADS 3 (27.8%), BI-RADS 4 (50%), and BI-RADS 5 (22.2%). Group 2: BI-RADS 3 (28.6%), BI-RADS 4 (47.6%), and BI-RADS 5 (23.8%).	SWV: Group 1, 1.98 ± 1.02 m/s; group 2, 2.82 ± 1.66 m/s.	Tozaki classification: Group 1: Pattern 1 (n=3), pattern 2 (n=5), pattern 3 (n=6), and pattern 4b (n=4); group 2: Pattern 1 (n=2), pattern 2 (n=3), pattern 3 (n=9), pattern 4a (n=1), and pattern 4b (n=6).
Makal and Guvenc (15)	Most common pattern: IGM: An irregular heterogeneous hypoechoic mass with tubular extensions. Malignancy: N/A. BI-RADS: IGM: 3.61 ± 0.65; Malignancy, 4.62 ± 0.49.	SWV: IGM: 2.5 ± 1.17 m/s; Malignancy: > 5 m/s.	SWE score: IGM: 3.07 ± 0.54; Malignancy, 4.62 ± 0.49.
Toprak et al. (16)	Most common pattern: IGM: Angular contours. Malignancy: Spiculated contours and posterior acoustic shadowing. All lesions: BI-RADS ≥ 4.	SWV: IGM: 3.78 ± 1.26 m/s; Malignancy, 5.34 ± 1.43 m/s.	Tozaki classification: IGM: Pattern 1 (n=9), pattern 2 (n=11), pattern 3 (n=17), and pattern 4a (n=2). Malignancy: Pattern 3 (n=15), pattern 4a (n=12), and pattern 4b (n=67).

Abbreviations: SR, strain ratio; IGM, idiopathic granulomatous mastitis; US, ultrasound; USE, ultrasound elastography; BI-RADS, breast imaging-reporting and data system; SWV, shear wave velocity; SWE, shear wave elastography; N/A, not applicable (or available).

Table 3. Evaluation of the Diagnostic Accuracy of Imaging Parameters in Distinguishing IGM from Breast Cancer

Authors	Diagnostic parameter	Diagnostic cut-off point	Sensitivity (%)	Specificity (%)	PPV	NPV	Accuracy (%)	AUC	Confounding factors	Number of operators and setting
Teke et al. (11)	SWV	4.07 m/s	91	91.7	96.5	80	91.2	N/A	N/A	2, N/A
Yagci et al. (12)	SR	2.5	87	96	N/A	N/A	N/A	0.939	Operator dependent	1, Blinded to the results
Arslan et al. (13)	Conventional US, ES, and US+ES	Conventional US: Category 3; ES: Score 3; SR: 2.71	Conventional US: 94.8; ES: 83.1; SR: 87; US+SR: 96.1; US+ES: 96.1	Conventional US: 66.7; ES: 100; SR: 100; US+SR: 100; US+ES: 100	Conventional US: 85.9; ES: 100; SR: 100; US+SR: 100; US+ES: 100	US: 85.7; ES: 73.5; SR: 78.3; US+SR: 92.3; US+ES: 92.3	Conventional US: 85.8; ES: 88.5; SR: 91.1; US+SR: 97.3; US+ES: 97.3	Conventional US: 0.80; ES: 0.91; SR: 0.97; US+SR: 0.98; US+ES: 0.98	Operator dependent	2, Blinded to the results
Makal and Guvenc (15)	SWV	4.1 m/s	97.5	93	92.6	97.6	95.2	0.94	Abscess in IGM may cause SWV to be lower.	1, N/A
Toprak et al. (16)	SWV	4.34 m/s	74	72	86	51	70	0.796	The size and central necrosis of malignant lesions may explain the incidence of pattern 3.	1, Blinded to the results

Abbreviations: AUC, area under the curve; PPV, positive predictive value; NPV, negative predictive value; SWV, shear wave velocity; SR, strain ratio; ES, elasticity score; US, ultrasound; IGM, idiopathic granulomatous mastitis; N/A, not applicable (or available).

and specificity of SWV in discriminating IGM from invasive ductal carcinoma (16). They reported 89% sensitivity and 84% specificity, based on the quantitative and qualitative findings of ARFI imaging. They also concluded that ARFI elastography could enhance the distinction between IGM and malignancies.

5. Discussion

The mammographic patterns of IGM can mimic other conditions, such as carcinoma, and are not exclusive for diagnosis (17). Areas of varied echogenicity, numerous and irregular hypoechoic masses, and heterogeneity of the parenchyma can be observed on US images (10-16). In various studies examining IGM lesions, the BI-RADS score, determined by B-mode US assessment, was found to be in the range of 3 - 5 (11, 13-16). Since IGM can resemble breast malignancies both clinically and radiologically, it is difficult to distinguish IGM from carcinomas using common diagnostic techniques, such as US imaging and mammography.

To differentiate between benign and malignant tumors, a biopsy is often required. However, this can lead to increased anxiety in patients and additional costs (18). Generally, USE is used to determine the stiffness of lesions. Due to their disorganized structure, cancerous tissues exhibit a different elasticity than anticipated. Therefore, practitioners employ palpation techniques to evaluate the

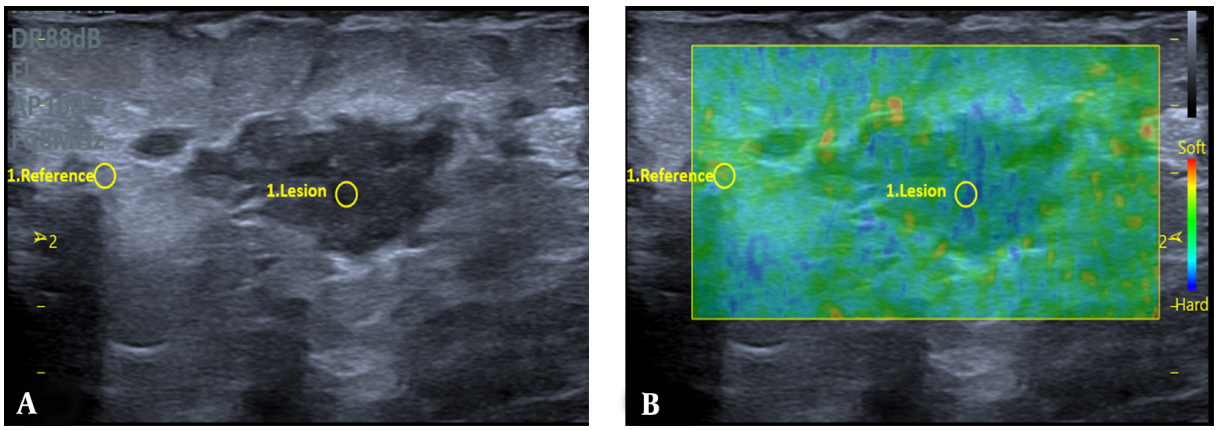

Figure 2. Grey-scale US (A) exhibits an irregular parallel mass with mild peripheral edema in a 29-year-old woman with a history of mastitis in the same breast over the past year. The strain elastography (B) indicates a strain ratio (SR) of 2.68, and the biopsy findings indicate an idiopathic granulomatous mastitis (IGM) lesion.

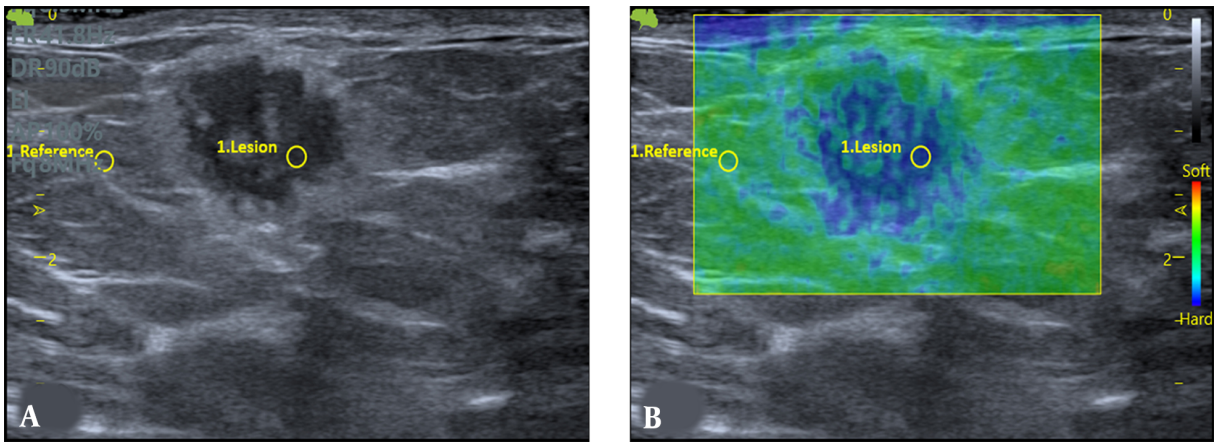

Figure 3. Grey-scale US (A) displays a round microlobulated mass with a thick halo in a 41-year-old woman. The mass appears stiff on strain elastography (B). The strain ratio (SR) is 4.76, and the lesion is shown to be invasive ductal carcinoma following core needle biopsy.

abnormal mass elasticity (7). USE is capable of detecting these disturbances in stiffness, aiding in the identification of malignant masses. The differentiation between benign and malignant lesions can potentially be achieved with higher sensitivity, specificity, and consistency using elastography (19). Figures 2 and 3 are examples of IGM and cancerous lesions on US and strain elastography.

The ES, SR, and elastic diameter (ED) of lesions are parameters of strain elastography. The Tsukuba ES is determined using Itoh's method (20). For each lesion, SR is determined by comparing the average strain of the lesion to that of the fat tissue in the same region at an equivalent depth. Moreover, ED is defined as the ratio of the B-mode and elastography diameters of the lesion (21). Compared to B-mode images, cancerous lesions appear larger on elastography. This is due to a desmoplastic response around tumors that can be detected by elastography, but may not be always visible on grey-scale US (22, 23). An indicator of cancer is a lesion that appears larger in diameter on elastography compared to US (23). On elastography, benign tumors typically exhibit the same diameter or a smaller one compared to US images. In this regard, Durur-Karakaya et al. (10) observed that the diameter of IGM was consistent on both grey-scale US and elastography.

Furthermore, Itoh et al. (20) found that malignant lesions have higher mean ES values compared to benign lesions (4.2 vs. 2.1). Additionally, Tan et al. (24) showed that in B-mode BI-RADS, categories 2 and 3 lesions had a lower median ES, while categories 4 and 5 lesions had a higher

overall median ES. Moreover, Cho et al. (25) suggested an SR cut-off value of 2.24 for differentiating benign from cancerous lesions. In their research, 95% of lesions had an SR value above 2.24. Also, Yagci et al. (12) and Arslan et al. (13) reported that IGM masses had significantly lower SR readings than malignancies. Further research has also revealed that the average SR of malignant lesions is higher than that of benign ones (23, 25).

Strain elastography employs manual compression, with the user applying pressure via the probe. Additionally, SWE is a dynamic elastography technique that utilizes shear waves generated by acoustic radiation force and is not dependent on the operator. Moreover, ARFI is a novel method that enables a qualitative analysis of tissue elasticity using virtual touch tissue imaging (VTI), as well as a quantitative analysis using virtual touch quantification (VTQ), without any need for compression. Compared to strain elastography, ARFI elastography has been found to have higher accuracy (26).

The VTI analysis provides a qualitative gray-scale mapping of relative tissue stiffness. Tozaki et al. (27) classified lesions into patterns 1, 2, 3, and 4, according to their VTI characteristics. Pattern 4 is subdivided into 4a and 4b, based on the size discrepancy between the VTI and B-mode images. Malignancies are predicted by a significant diameter gap in VTI compared to the B-mode views. Teke et al. (11) reported that none of the IGM lesions fell into the 4b pattern category, and all instances of the 4b pattern were identified as malignant. Also, in a study by Toprak et al. (16), none of the IGM lesions showed a 4b pattern.

Additionally, Makal and Guvenc (15) found that according to US BI-RADS, IGM lesions are predominantly classified in group 4. Following elastography, the median Tsukuba score was measured to be three for IGM lesions, while for malignant lesions, the US BI-RADS and Tsukuba scores were found to be in agreement (both 5). While Aslan et al. (14) found that 25% of IGM lesions (10/39) exhibited a 4b pattern, other studies (11, 16) found that all lesions with a 4b pattern were malignant. These results indicate that pattern 4 subtypes are important from a clinical standpoint. The VTI of breast malignancies typically exhibits a 4b pattern. This is often due to peritumoral invasion and the desmoplastic reaction associated with these malignancies.

Moreover, VTQ is a quantitative ARFI technology used to measure SWV (28). Teke et al. (11) reported substantial variance in the marginal and internal SWV values between IGM and cancerous lesions. In addition, Toprak et al. (16) demonstrated that the mean SWV of IGM lesions was significantly lower than that of malignancies. Overall, relying solely on a quantitative technique can lead to false-positive findings, despite the fact that VTQ has a high diagnostic accuracy in distinguishing IGM from malignancies. This is because previous studies have indicated that IGM lesions exhibit high SWV values, which may be similar to those of malignancies (29, 30).

The majority of biopsy recommendations are derived from BI-RADS 4. On US images, lower PPVs are typically associated with BI-RADS 4 lesions, leading to additional biopsies (31). While in previous studies, some malignant lesions were classified as patterns 4a and 3 (11, 15, 16), the combined use of VTI and VTQ could potentially enhance the accuracy of diagnosing malignancies. In the study by Teke et al. (11), compared to IGM lesions categorized into patterns 3 or 4a, the average SWV of malignancies was found to be higher in these patterns. Furthermore, when the results of VTI were combined with those of VTQ for the evaluation of these patterns, the diagnostic parameters showed significant improvement.

This study has some limitations. Interestingly, all the studies conducted in this field have been carried out in Turkey, which has the highest number of IGM patients globally (32). Therefore, to generalize the results, it is necessary to perform this investigation in other regions to assess patients of different races. One significant challenge in replicating these studies and establishing a definitive cut-off value may be the rarity of IGM cases in other countries. However, as the use of elastography becomes increasingly important in diagnosing breast masses, the necessary data for such studies is becoming more accessible. Indeed, there is still a significant need for more extensive research in this field. Despite the limitations mentioned, this review represents the first systematic study on this subject, and its findings can motivate future research endeavors.

In conclusion, the B-mode view of IGM lesions can often resemble that of malignant lesions. Therefore, a major concern for both clinicians and patients is ensuring an accurate diagnosis and avoiding unnecessary biopsies for these lesions. An examination of the USE parameters for IGM lesions can reveal the unique characteristics of these lesions, potentially improving the accuracy of diagnosis. This review demonstrated that the diagnostic intervals proposed for USE parameters (SWV = 4.07 - 4.34 m/s, SR = 2.50 - 2.71) may be useful in the diagnosis of IGM lesions and their discrimination from breast cancer. The application of this modality can potentially reduce the number of unnecessary biopsies to differentiate IGM from breast cancer.

Acknowledgments

Solely the authors contributed to this review, with no external assistance.

Footnotes

Authors' Contributions: Study concept and design: M.G. and S.M.H.; Acquisition of data: M.A.A., S.M.H., and A.J.; Analysis and interpretation of data: S.M.H., M.G., M.A.A., and P.T.B.; Drafting of the manuscript: S.M.H., A.J., and P.T.B.; Critical revision of the manuscript for important intellectual content: M.G. and P.T.B.; Study supervision: M.G.

Conflict of Interests: The authors declare no financial or personal conflicts of interest.

Data Reproducibility: The dataset presented in the study is available on request from the corresponding author during submission or after publication.

Funding/Support: The authors received no funding for this article.

References

1. Yin Y, Liu X, Meng Q, Han X, Zhang H, Lv Y. Idiopathic Granulomatous Mastitis: Etiology, Clinical Manifestation, Diagnosis and Treatment. *J Invest Surg*. 2022;**35**(3):709–20. [PubMed ID: 33691563]. https://doi.org/10.1080/08941939.2021.1894516.
2. Kessler E, Wolloch Y. Granulomatous mastitis: a lesion clinically simulating carcinoma. *Am J Clin Pathol*. 1972;**58**(6):642–6. [PubMed ID: 4674439]. https://doi.org/10.1093/ajcp/58.6.642.
3. Eryilmaz N, Eryilmaz MA, Arslan S, Solak I, Pekgor S, Altunkeser A, et al. Clinical and Radiological Differences Between Fistular and Non-Fistular Idiopathic Granulomatous Mastitis. *Iran J Radiol*. 2018;**In Press**(In Press). https://doi.org/10.5812/iranjradiol.79333.
4. Gautier N, Lalonde L, Tran-Thanh D, El Khoury M, David J, Labelle M, et al. Chronic granulomatous mastitis: Imaging, pathology and management. *Eur J Radiol*. 2013;**82**(4):e165–75. [PubMed ID: 23200627]. https://doi.org/10.1016/j.ejrad.2012.11.010.
5. Barreto DS, Sedgwick EL, Nagi CS, Benveniste AP. Granulomatous mastitis: etiology, imaging, pathology, treatment, and clinical findings. *Breast Cancer Res Treat*. 2018;**171**(3):527–34. [PubMed ID: 29971624]. https://doi.org/10.1007/s10549-018-4870-3.
6. Poyraz N, Emlik GD, Batur A, Gundes E, Keskin S. Magnetic Resonance Imaging Features of Idiopathic Granulomatous Mastitis: A Retrospective Analysis. *Iran J Radiol*. 2016;**13**(3). e20873. [PubMed ID: 27853486]. [PubMed Central ID: PMC5106557]. https://doi.org/10.5812/iranjradiol.20873.
7. Sigrist RMS, Liau J, Kaffas AE, Chammas MC, Willmann JK. Ultrasound Elastography: Review of Techniques and Clinical Applications. *Theranostics*. 2017;**7**(5):1303–29. [PubMed ID: 28435467]. [PubMed Central ID: PMC5399595]. https://doi.org/10.7150/thno.18650.
8. Page MJ, McKenzie JE, Bossuyt PM, Boutron I, Hoffmann TC, Mulrow CD, et al. The PRISMA 2020 statement: an updated guideline for reporting systematic reviews. *BMJ*. 2021;**372**:n71. [PubMed ID: 33782057]. [PubMed Central ID: PMC8005924]. https://doi.org/10.1136/bmj.n71.
9. Aromataris E, Munn Z. *JBI Manual for Evidence Synthesis*. JBI; 2020. Available from: https://synthesismanual.jbi.global..
10. Durur-Karakaya A, Durur-Subasi I, Akcay MN, Sipal S, Guvendi B. Sonoelastography findings for idiopathic granulomatous mastitis. *Jpn J Radiol*. 2015;**33**(1):33–8. [PubMed ID: 25466769]. https://doi.org/10.1007/s11604-014-0378-x.
11. Teke M, Teke F, Alan B, Turkoglu A, Hamidi C, Goya C, et al. Differential diagnosis of idiopathic granulomatous mastitis and breast cancer using acoustic radiation force impulse imaging. *J Med Ultrason (2001)*. 2017;**44**(1):109–15. [PubMed ID: 27787642]. https://doi.org/10.1007/s10396-016-0749-2.
12. Yagci B, Erdem Toslak I, Cekic B, Oz M, Karakas BR, Akdemir M, et al. Differentiation between idiopathic granulomatous mastitis and malignant breast lesions using strain ratio on ultrasonic elastography. *Diagn Interv Imaging*. 2017;**98**(10):685–91. [PubMed ID: 28729183]. https://doi.org/10.1016/j.diii.2017.06.009.
13. Arslan S, Oncu F, Eryilmaz MA, Durmaz MS, Altunkeser A, Unlu Y. Advantages of b-mode ultrasound combined with strain elastography in differentiation of idiopathic granulomatous mastitis from malignant breast lesions. *Turk J Med Sci*. 2018;**48**(1):16–23. [PubMed ID: 29479939]. https://doi.org/10.3906/sag-1708-34.
14. Aslan H, Arer IM, Pourbagher A, Ozen M. Is there a correlation between the severity of Idiopathic Granulomatous Mastitis and pre-treatment Shear-Wave Elastography Findings? Original research. *Ann Ital Chir*. 2018;**89**:489–94. [PubMed ID: 30665211].
15. Makal GB, Guvenc I. The Role of Shear Wave Elastography in Differentiating Idiopathic Granulomatous Mastitis From Breast Cancer. *Acad Radiol*. 2021;**28**(3):339–44. [PubMed ID: 32217054]. https://doi.org/10.1016/j.acra.2020.02.008.
16. Toprak N, Toktas O, Ince S, Gunduz AM, Yokus A, Akdeniz H, et al. Does ARFI elastography complement B-mode ultrasonography in the radiological diagnosis of idiopathic granulomatous mastitis and invasive ductal carcinoma? *Acta Radiol*. 2022;**63**(1):28–34. [PubMed ID: 33377394]. https://doi.org/10.1177/0284185120983568.
17. Woodard GA, Bhatt AA, Knavel EM, Hunt KN. Mastitis and More: A Pictorial Review of the Red, Swollen, and Painful Breast. *J Breast Imaging*. 2021;**3**(1):113–23. https://doi.org/10.1093/jbi/wbaa098.
18. Hovanessian Larsen LJ, Peyvandi B, Klipfel N, Grant E, Iyengar G. Granulomatous lobular mastitis: imaging, diagnosis, and treatment. *AJR Am J Roentgenol*. 2009;**193**(2):574–81. [PubMed ID: 19620458]. https://doi.org/10.2214/AJR.08.1528.
19. Barr RG, Destounis S, Lackey L, Svensson WE, Balleyguier C, Smith C. Evaluation of breast lesions using sonographic elasticity imaging: a multicenter trial. *J Ultrasound Med*. 2012;**31**(2):281–7. [PubMed ID: 22298872]. https://doi.org/10.7863/jum.2012.31.2.281.
20. Itoh A, Ueno E, Tohno E, Kamma H, Takahashi H, Shiina T, et al. Breast disease: clinical application of US elastography for diagnosis. *Radiology*. 2006;**239**(2):341–50. [PubMed ID: 16484352]. https://doi.org/10.1148/radiol.2391041676.
21. Franchi-Abella S, Elie C, Correas JM. Ultrasound elastography: advantages, limitations and artefacts of the different techniques from a study on a phantom. *Diagn Interv Imaging*. 2013;**94**(5):497–501. [PubMed ID: 23567179]. https://doi.org/10.1016/j.diii.2013.01.024.
22. Balleyguier C, Ciolovan L, Ammari S, Canale S, Sethom S, Al Rouhbane R, et al. Breast elastography: the technical process and its applications. *Diagn Interv Imaging*. 2013;**94**(5):503–13. [PubMed ID: 23619293]. https://doi.org/10.1016/j.diii.2013.02.006.
23. Goddi A, Bonardi M, Alessi S. Breast elastography: A literature review. *J Ultrasound*. 2012;**15**(3):192–8. [PubMed ID: 23449849]. [PubMed Central ID: PMC3558110]. https://doi.org/10.1016/j.jus.2012.06.009.
24. Tan SM, Teh HS, Mancer JF, Poh WT. Improving B mode ultrasound evaluation of breast lesions with real-time ultrasound elastography–a clinical approach. *Breast*. 2008;**17**(3):252–7. [PubMed ID: 18054231]. https://doi.org/10.1016/j.breast.2007.10.015.

25. Cho N, Moon WK, Kim HY, Chang JM, Park SH, Lyou CY. Sonoelastographic strain index for differentiation of benign and malignant nonpalpable breast masses. *J Ultrasound Med*. 2010;**29**(1):1–7. [PubMed ID: 20040770]. https://doi.org/10.7863/jum.2010.29.1.1.
26. Kim YS, Park JG, Kim BS, Lee CH, Ryu DW. Diagnostic value of elastography using acoustic radiation force impulse imaging and strain ratio for breast tumors. *J Breast Cancer*. 2014;**17**(1):76–82. [PubMed ID: 24744801]. [PubMed Central ID: PMC3988346]. https://doi.org/10.4048/jbc.2014.17.1.76.
27. Tozaki M, Isobe S, Sakamoto M. Combination of elastography and tissue quantification using the acoustic radiation force impulse (ARFI) technology for differential diagnosis of breast masses. *Jpn J Radiol*. 2012;**30**(8):659–70. [PubMed ID: 22836905]. https://doi.org/10.1007/s11604-012-0106-3.
28. Ianculescu V, Ciolovan LM, Dunant A, Vielh P, Mazouni C, Delaloge S, et al. Added value of Virtual Touch IQ shear wave elastography in the ultrasound assessment of breast lesions. *Eur J Radiol*. 2014;**83**(5):773–7. [PubMed ID: 24602803]. https://doi.org/10.1016/j.ejrad.2014.01.021.
29. Sousaris N, Barr RG. Sonographic Elastography of Mastitis. *J Ultrasound Med*. 2016;**35**(8):1791–7. [PubMed ID: 27353071]. https://doi.org/10.7863/ultra.15.09041.
30. Yoon JH, Jung HK, Lee JT, Ko KH. Shear-wave elastography in the diagnosis of solid breast masses: what leads to false-negative or false-positive results? *Eur Radiol*. 2013;**23**(9):2432–40. [PubMed ID: 23673572]. https://doi.org/10.1007/s00330-013-2854-6.
31. Athanasiou A, Tardivon A, Tanter M, Sigal-Zafrani B, Bercoff J, Deffieux T, et al. Breast lesions: quantitative elastography with supersonic shear imaging–preliminary results. *Radiology*. 2010;**256**(1):297–303. [PubMed ID: 20505064]. https://doi.org/10.1148/radiol.10090385.
32. Metanat S, Soleimani Jobaneh Y, Noori M, Sadeghi F, Mirzapour A, Mashoori N, et al. Global Distribution of Idiopathic Granulomatous Mastitis: A Scoping Review. *Arch Breast Cancer*. 2022;**9**(3-SI):261–71. https://doi.org/10.32768/abc.20229SI261-271.